# Jahn-Teller effects in the mixed vanadate/phosphate crystals $TbV_{1-x}P_xO_4$ $(0 \leqslant x \leqslant 0.32)$

Y. Hirano,[1] N. Wakabayashi,[1] C.-K. Loong,[2] and L. A. Boatner[3]
[1]*Department of Physics, Keio University, Yokohama 223-8522, Japan*
[2]*Intense Pulsed Neutron Division, Argonne National Laboratory, Argonne, Illinois 60439*
[3]*Solid State Division, Oak Ridge National Laboratory, Oak Ridge, Tennessee 37831*
(Received 12 October 2002; published 31 January 2003)

X-ray-diffraction measurements were performed on mixed vanadate/phosphate single crystals of the type: $TbV_{1-x}P_xO_4$ (where $x=0$, 0.10, 0.18, 0.24, and 0.32) in order to investigate the effects of P doping on the Jahn-Teller phase transition. The transition temperature, below which the tetragonal symmetry of the lattice is lowered to orthorhombic, decreases with increasing P concentration. In order to explain the order parameters of the transition and the striking reduction in the transition temperature with increasing P content, a modified mean-field model was developed for the mixed system. A simple calculation assuming only a distribution in the value of the quadrupolar crystal-field parameter $B_2^0$ is unsatisfactory. Since the local tetragonal symmetry is broken due to the random distribution of phosphorous, a term involving the operator $P_{xy}=\frac{1}{2}(J_xJ_y+J_yJ_x)$ was introduced in the Hamiltonian that includes both the crystal-field and magnetoelastic effects. This term, in conjunction with the distribution in the magnitude of the corresponding crystal-field parameter, was essential in order to reproduce the observed temperature dependence of the order parameter (orthorhombic strain). The results of the diffuse scattering measurements performed on the $x=0.32$ crystal confirmed the existence of local strains that should give rise to variation in $B_2^0$. The diffuse intensity due to strains having the symmetry associated with $P_{xy}$ could not be resolved, however, because of the overlapping thermal diffuse scattering.

DOI: 10.1103/PhysRevB.67.014423 PACS number(s): 75.50.−y, 46.25.Hf, 61.50.Ks

## I. INTRODUCTION

Rare-earth vanadates $RVO_4$ and arsenates $RAsO_4$ ($R$ = rare-earth elements) crystallize in the tetragonal zircon structure (space group $D_{4h}^{19}$ *or* $I4_1/amd$ No. 141) at room temperature.[1,2] There are two formula units per unit cell in which the rare-earth ions occupy an equivalent site of $D_{2d}$ symmetry. Some of these compounds undergo a cooperative Jahn-Teller phase transition at low temperatures. In $TbVO_4$, $TbAsO_4$, $TmVO_4$, and $TmAsO_4$, the Jahn-Teller transition, associated with an orthorhombic distortion of $B_{2g}$ symmetry, occurs at 33, 27.7, 2.10, and 6.1 K, respectively.[3] The orthorhombic axes $a_o$ and $b_o$ are parallel to the bisectors of the tetragonal $a_t$ and $b_t$ axes. The phase transitions of $DyVO_4$ and $DyAsO_4$ at 14.0 and 11.2 K, respectively, are accompanied by an orthorhombic $B_{1g}$ distortion whereby $a_o$ and $b_o$ axes are parallel to $a_t$ and $b_t$, respectively.[3]

Among the series of rare-earth phosphates $RPO_4$ only $TbPO_4$ exhibits a Jahn-Teller phase transition. $TbPO_4$ crystallizes in the same tetragonal zircon structure as that of the $RVO_4$ and $RAsO_4$ compounds at room temperature.[2] In the case of $TbPO_4$, an antiferromagnetic ordering occurs below 2.28 K with the rare-earth magnetic moments lying parallel to the tetragonal $c$ axis.[4] The magnetic phase transition is followed by a Jahn-Teller structural transition at 2.15 K. At this point, the lattice distorts to a monoclinic structure, and simultaneously, the magnetic moments tilt away from the $c$ axis in the (110) plane.

Jahn-Teller transitions in the vanadates and arsenates containing two different rare-earth cations have been studied previously.[5–17] In general, a reduction of the transition temperature $T_D$ was observed in these mixed compounds. A modified molecular-field model was developed to explain the experimental data. In some cases, introducing the effect of localized random strains corresponding to the symmetry of the Jahn-Teller distortion was essential to a proper interpretation of the experimental results.[6,10–12] Such strains would exist, in principle, at all temperatures due to the effects of chemical doping.

Doping a nonmagnetic cation in a $RVO_4$ has a different type of effect on both the Jahn-Teller transition and the magnetic properties. Some studies of the critical exponents in $R(V,As)O_4$ ($R$=Tb, Dy, Tm) in the framework of a random-field Ising model have been reported.[18–21] However, reports on mixed compounds with V and P are relatively few. Within the lanthanide series $RPO_4$ forms the tetragonal zircon structure (xenotime) only for the heavy rare-earth members (from Tb to Lu). Additionally, the crystal growth of $R(V,P)O_4$ is complicated due to the relatively large difference in the ionic radius between the V and P. Specifically, the magnetic properties of $Dy(V,P)O_4$ were investigated previously, and a crossover from the antiferromagnetic ordering at the V- and P-rich ends to a spin-glass state in the intermediate-concentration range was found at low temperatures.[22] Additionally, Skanthakumar *et al.* have reported the results of a neutron-scattering study of the anomalous thermal expansion in $Ho(V,P)O_4$.[23] Studies of the Jahn-Teller transition in the $R(V,P)O_4$ have apparently not been carried out previously, and the present work presents the results of an investigation of Jahn-Teller effects in the case of the mixed vanadate/phosphate $TbV_{1-x}P_xO_4$.

The splitting of the $Tb^{3+}$:$^7F_6$ ground multiplet of $TbVO_4$ by the crystal-field (CF) has been reported by many authors.[24,25] The Hamiltonian for a single-ion CF model for a rare-earth ion occupying the tetragonal-symmetry site contains five terms. The second-order (quadrupolar) term can be written as $\alpha B_2^0 O_2^0$, where $\alpha$ is the Stevens factor, $B_n^m$ the CF parameter, and $O_n^m$ the operator equivalent.[26] The $B_2^0$ CF pa-

 

rameter determines, to a large extent, the symmetry of the wave functions of the ground and low-lying states, and in turn, the symmetry manifests itself in the anisotropy of the magnetic susceptibility at low temperatures.

For $TbVO_4$, both $\alpha$ and $B_2^0$ are negative, and hence, the quadrupolar term of the CF Hamiltonian favors the states with a large angular momentum component in the basal plane. At temperatures near $T_D$, only the four low-lying states (two singlets, $\Gamma_1$ and $\Gamma_3$, and one $\Gamma_5$ doublet) are thermally populated and contribute to the Jahn-Teller effect.[25] The $\Gamma_3$ singlet is $\approx 18\ cm^{-1}$ above the $\Gamma_1$ ground state, and a $\Gamma_5$ doublet lies near the midpoint between the singlet levels. The Jahn-Teller phase transition is driven by the coupling between these electronic states and a lattice distortion of $B_{2g}$ symmetry, resulting in an increase in the spacing between the $\Gamma_1$ and $\Gamma_3$ levels and in a large splitting of the $\Gamma_5$ doublet below $T_D$.

The difference in the CF between the phosphates and vanadates for a given rare-earth ion is represented by an opposite sign of the quadrupolar CF parameter $B_2^0$. Accordingly, the $\Gamma_5$ ground state of the Tb ion in $TbPO_4$ has large $J_z$ components (consisting mainly of $|J=6,J_z=\pm 5\rangle$)[27] with the quantization axis coincident with the crystallographic $c$ direction. The degeneracy of the ground-state $\Gamma_5$ doublet is lifted by the monoclinic distortion below $T_D$.

A traditional way of describing the Jahn-Teller effects in $TbVO_4$ is the pseudospin formalism put forth by Elliott *et al.*[25] This formalism considers only the four low-lying states, and the Hamiltonian is expressed in $4\times 4$ Pauli spin matrices. It is postulated in this theory that the wave functions of these four states can be written by linear combinations of the states: $|J=6,J_x=\pm J\rangle$ and $|J=6,J_y=\pm J\rangle$. In the studies on mixed compounds in which a fraction of the Tb ions is replaced by other rare-earth ions, the model has been extended to take into account randomness within the framework of the pseudospin formalism.[10–12,17] However, since doping with P ions is expected to create a CF that favors an easy magnetization along the $c$ axis, the pseudospin formalism, which is based on the four low-lying states of $TbVO_4$ consisting of $J_z$ components in the basal plane, is not adequate to describe the Jahn-Teller effects in $TbV_{1-x}P_xO_4$.

In the present work, the structural properties of the mixed compounds $TbV_{1-x}P_xO_4$ were investigated by x-ray diffraction. The temperature dependence of the $B_{2g}$ orthorhombic distortion, which is the order parameter of the transition, was measured for samples with various P concentrations. Based on these data, the effect of randomness caused by the P doping on cooperative phenomena such as the Jahn-Teller transition is discussed without resorting to the pseudospin formalism.

## II. EXPERIMENTAL DETAILS

Single crystals of $TbV_{1-x}P_xO_4$ were prepared by flux-growth methods as described previously.[28] The crystals have the shape of a rectangular parallelepiped with the long dimension along the crystallographic $c$ direction. Typical sample dimensions are $1\times 1\times 4\ mm^3$. The composition of the five samples was measured by inductively coupled plasma-atomic emission spectrometry using a Perkin Elmer optima 3300 dual view spectrometer system with an accuracy of 3–5 % in the measured value of the relative P/V ratio.

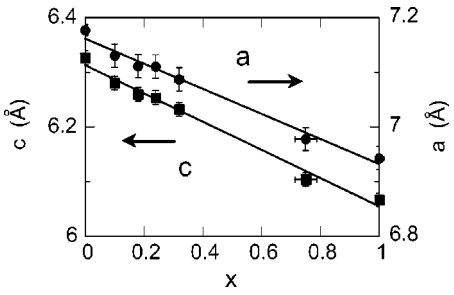


FIG. 1. The lattice parameters $a_t$ and $c_t$ at room temperature as a function of the concentration $x$. The straight lines are fits to a linear dependence with $x$.

X-ray diffraction experiments were performed using a conventional diffractometer with a Cu $K_\alpha$ radiation source. The samples were cooled using a closed-cycle helium refrigerator, and the temperature was controlled to within 0.5 K. To observe the Jahn-Teller phase transition, the temperature dependence of the (660) Bragg reflection was monitored. At $T_D$, the reflection splits into two lines, i.e., (12,0,0) and (0,12,0) reflections of the orthorhombic phase, due to twinning.[29] The lattice parameters were determined by measuring the peak positions of Bragg reflections such as (800), (008), (660), and (107) for the tetragonal phase, and (12,0,0) and (0,12,0) for the orthorhombic phase. The size of the orthorhombic distortion can be obtained from the values of the orthorhombic lattice constants $a_o$ and $b_o$. In order to observe diffuse scattering arising from the local lattice distortions, the intensity of the scattered x ray was measured around the tetragonal (660) reflection in the $\{hk0\}$ reciprocal plane.

## III. EXPERIMENTAL RESULTS

### A. Jahn-Teller phase transition

The lattice parameters $a_t$ and $c_t$ were determined at room temperature by measuring the peak positions of several $(h0l)$ reflections. Their $x$ dependence is shown in Fig. 1. The lines in Fig. 1 are the result of a linear fit. The error bars represent the scattered values of the lattice constants obtained for different $(h0l)$ reflections and for different sample alignments. The lattice constants of $TbV_{1-x}P_xO_4$ vary linearly over the full range of concentration $0\leqslant x\leqslant 1$. A similar linear behavior of the lattice constants as well as of the oxygen positions was reported previously for $HoV_{1-x}P_xO_4$.[23]

The temperature dependence of the tetragonal (660) reflection was observed for the $TbV_{1-x}P_xO_4$ crystals as the temperature was lowered from room temperature. The splitting of the Bragg peak, indicating the onset of structural change from tetragonal to orthorhombic, was observed at $33\pm 0.5$, $28.5\pm 0.5$, $23.5\pm 0.5$, $23.5\pm 0.5$, and $18\pm 0.5$ K for $x=0$, 0.10, 0.18, 0.24, and 0.32, respectively. No evidence

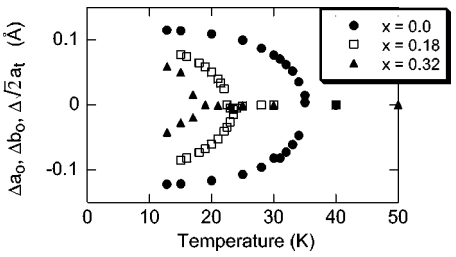


FIG. 2. The temperature dependences of $a_o$, $b_o$ and $\sqrt{2}a_t$ relative to the value of $\sqrt{2}a_t$ at 40 K for each value of $x$.

of the phase transition was observed for $x=0.75$ down to $T=12$ K. The lattice constants $a_o$ and $b_o$ were determined from the positions of the (12,0,0) and (0,12,0) peaks. Figure 2 shows temperature dependence of $a_o$, $b_o$, and $\sqrt{2}a_t$ relative to the value of $\sqrt{2}a_t$ at $T=40$ K for each $x$ value.

The order parameter of the Jahn-Teller phase transition is the $B_{2g}$ orthorhombic distortion $\varepsilon_{\mathrm{JT}}^{\delta}$ determined from the measured values of $a_o$ and $b_o$ as:

$$\varepsilon_{\mathrm{JT}}^{\delta}=\sqrt{2}\frac{a_o-b_o}{a_o+b_o}. \tag{1}$$

The order parameter as a function of temperature for $x=0$, 0.10, 0.18, 0.24, and 0.32 is shown in Fig. 3.

### B. Diffuse scattering

In the mixed crystals, the CF experienced by the Tb ions will be modified by the random substitution of V by P. It is likely that a part of this modification is caused by displacements of the neighboring ions around the Tb ion, i.e., local strains in the lattice. In order to determine if such strains exist, we have to first establish the normal thermal diffuse scattering (TDS) pattern of the samples. The TDS patterns, such as that shown in Fig. 4(a), can be calculated[30] using the elastic constants of $TbVO_4$,[31] and the intensity is expected to decrease with decreasing temperature. Experimentally, the TDS was verified by measurements of the diffuse scattering from a pure $TbVO_4$ crystal. Next, the extra component of diffuse scattering due to local lattice strains, if present, can

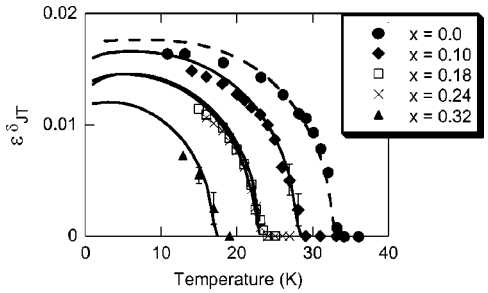


FIG. 3. The temperature dependences of the order parameter $\varepsilon_{\mathrm{JT}}^{\delta}$ for $x=0$, 0.10, 0.18, 0.24, and 0.32. The dashed line represents the calculated values for pure $TbVO_4$. The solid lines represent results of the calculation assuming the distribution in $B_{xy}$. The values of $B_{xy-half}$ chosen for $x=0.10$, 0.18, 0.24, and 0.32 are 56, 74, 73, and 87 $\mathrm{cm}^{-1}$, respectively (see text for the definition of $B_{xy-half}$).

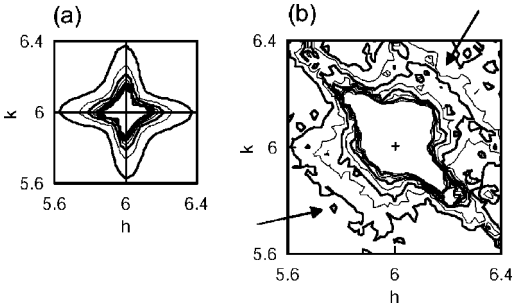


FIG. 4. (a) The calculated intensity distribution of the thermal diffuse scattering around the (660) reflection. (b) The measured intensity distribution of the diffuse scattering around the (660) reflection for the $x=0.32$ crystal at room temperature.

be identified. For example, the contour plot of the measured diffuse scattering intensity around the (660) reflection in the $\{hk0\}$ reciprocal plane for $x=0.32$ at room temperature is shown in Fig. 4(b). The distribution of the intensity extending along the $(1\bar{1}0)$ direction is due to the mosaic structure of the sample. For $x=0.32$, a distinctive diffuse scattering intensity was observed in the $h>6$, $k>6$, and $h<6$, $k<6$ regions as indicated by the arrows in Fig. 4(b). It differs clearly from that of the TDS. The diffuse scattering that is unique to the mixed crystals presumably arises from the local strains caused by the incorporation of P atoms. A detailed analysis of the diffuse scattering pattern will be presented in Sec. IV C.

## IV. ANALYSIS AND DISCUSSION

### A. Crystal-field and magnetoelastic coupling Hamiltonian

The CF Hamiltonian is expressed according to the Steven's operator equivalent method.[26] We adopt the notation used by Kazei and co-workers in the calculation of the temperature dependences of the lattice constants for $TbVO_4$.[32] The CF Hamiltonian is written as

$$H_{CF}=\alpha B_2^0 O_2^0+\beta(B_4^0 O_4^0+B_4^4 O_4^4)+\gamma(B_6^0 O_6^0+B_6^4 O_6^4). \tag{2}$$

The driving mechanism of the Jahn-Teller phase transition is the spin-lattice interaction, which may be approximated by a magnetoelastic coupling Hamiltonian. The lowest-order and most-dominant terms of the magnetoelastic Hamiltonian take the following form:

$$H_{ME}=-\alpha(B^{\alpha 1}\varepsilon^{\alpha 1}+B^{\alpha 2}\varepsilon^{\alpha 2})O_2^0-\alpha B^{\delta}\varepsilon^{\delta}P_{xy}, \tag{3}$$

where $\varepsilon^{\mu}$ ($\mu=\alpha 1,\alpha 2,\delta$) are the symmetrized strains defined in Ref. 33. The strains $\varepsilon^{\alpha 1}$ and $\varepsilon^{\alpha 2}$ retain the tetragonal symmetry of the lattice—the former represents the change in volume and the latter the change in the $c/a$ ratio. The strain $\varepsilon^{\delta}$ ($\sqrt{2}\varepsilon_{xy}$ in the Cartesian notation)[33] is the orthorhombic deformation, and the operator that couples to the strain of this symmetry is $P_{xy}$ defined as $\frac{1}{2}(J_xJ_y+J_yJ_x)$. Within the mean-field approximation, the Hamiltonian of the two-ion quadrupolar interaction can be written as

TABLE I. A comparison of the measured (Ref. 36) and calculated low-lying energy levels (in units of $cm^{-1}$) for $TbVO_4$. The $\Gamma_5$ states are doubly degenerate and the others are singlets.

| (a) just above $T_D$ (tetragonal) | | | (b) at 6 K (orthorhombic) | | |
|---|---|---|---|---|---|
| symmetry | measured | calculated | symmetry | measured | calculated |
| $\Gamma_5$ | $88.7\pm1.5$ | 88.8 | $\Gamma_2$ | $93.9\pm2$ [a] | 110.2 [b] |
| | | | $\Gamma_4$ | $90.2\pm2$ [a] | 97.7 [b] |
| $\Gamma_3$ | $19.1\pm0.5$ | 19.1 | $\Gamma_1$ | $51.3\pm0.5$ | 49.7 |
| $\Gamma_5$ | $8.0\pm0.5$ | 8.0 | $\Gamma_2$ | $47.9\pm0.7$ | 45.7 |
| | | | $\Gamma_4$ | $0.9\pm0.2$ | 0.65 |
| $\Gamma_1$ | 0 | 0 | $\Gamma_1$ | 0 | 0 |

[a]Data measured at 16 K from Ref. 25.
[b]Calculated for $T=16$ K.

$$H_Q=-\alpha^2(K^\alpha\langle O_2^0\rangle O_2^0-K^\delta\langle P_{xy}\rangle P_{xy}). \tag{4}$$

The elastic energy is expressed in terms of symmetrized elastic constants $C_0^{\alpha i}$'s and $C_0^\delta$ as follows:

$$E_{el}=\frac{1}{2}C_0^{\alpha1}(\varepsilon^{\alpha1})^2+C_0^{\alpha12}\varepsilon^{\alpha1}\varepsilon^{\alpha2}+\frac{1}{2}C_0^{\alpha2}(\varepsilon^{\alpha2})^2 + \frac{1}{2}C_0^{\delta}(\varepsilon^{\delta})^2. \tag{5}$$

By minimizing the free energy with respect to the strains, one can show that the equilibrium strains $\varepsilon^\mu$ are proportional to the expectation values of the corresponding quadrupolar operators. For example, the orthorhombic strain $\varepsilon^\delta$ is proportional to $\langle P_{xy}\rangle$. By replacing the strains $\varepsilon^\mu$'s in Eq. (3) with the expectation values of the operators, one can combine Eqs. (3) and (4) to define the total coupling Hamiltonian as

$$H_{coupling}=-\alpha^2(G^\alpha\langle O_2^0\rangle O_2^0-G^\delta\langle P_{xy}\rangle P_{xy}). \tag{6}$$

Since the coupling via acoustic phonons is dominant in the two-ion pair quadrupolar interaction in $TbVO_4$,[31] it can be shown that the renormalized coupling constant $G^\alpha$ can be expressed in terms of $B^{\alpha I}$ and $C_0^{\alpha i}$.[34] Before analyzing the Jahn-Teller effect in mixed crystals, the values of the CF parameters of the Tb ions in $TbVO_4$ are required. In order to account for the Jahn-Teller transition of the type found in $TbVO_4$, the matrix element of the operator $P_{xy}$ between the $\Gamma_1$ ground state and the $\Gamma_3$ singlet above $T_D$ must be relatively large. A calculation using the CF parameters estimated previously (based on the magnetic susceptibility of a powder sample)[35] did not reproduce the Jahn-Teller transition with the $B_{2g}$ distortion. Consequently, we searched for a new parameter set that produced an energy-level scheme and magnetic susceptibility that are consistent with the experimental data above $T_D$.[36,37] The low-lying energy levels observed in optical spectroscopy at a temperature just above $T_D$ and at 6 K were reported in Ref. 36 and are listed in Table I. The energies for the upper $\Gamma_2$ and $\Gamma_4$ states below $T_D$ obtained by Raman measurements[25] are included in the table. The magnetic susceptibility of a $TbVO_4$ crystal grown by the same method was measured with the magnetic field parallel and perpendicular to the tetragonal $c$ axis,[37] and the data are shown in Fig. 5. The phase transition does not affect the susceptibility along the tetragonal $a$ axis. Anomalies were observed in the susceptibility measured along the $c$ axis and along the bisector of tetragonal $a_t$ and $b_t$ axes.[38] We have obtained the set of CF parameters given in Table II. As can be seen from Table I, the calculated energy levels are in good agreement with those observed optically above $T_D$. The calculation was performed for $T<T_D$ using magnetoelastic coefficients determined from the analysis described in the following section and the calculated energy levels are given in Table I. The calculated magnetic susceptibility indicated by solid lines in Fig. 5 are also in good agreement with the observation except for $\chi_{\|c}$ below $T_D$. This discrepancy may be due to the omission of the higher-order CF parameters such as $B_4^2$ and $B_6^2$ for the orthorhombic symmetry, but we consider the parameter set in Table II can be used as a basis for discussion of the Jahn-Teller transition in $TbVO_4$.

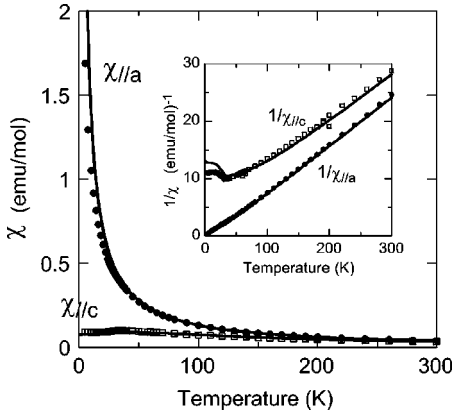


FIG. 5. The calculated (lines) and measured (symbols) paramagnetic susceptibility of $TbVO_4$ with the applied magnetic field parallel to the tetragonal $a$ axis and $c$ axis. Inset shows the inverse susceptibility.

### B. Jahn-Teller phase transition

In order to analyze the data on the basis of the magnetoelastic coupling, one needs the information about the elastic constants of the tetragonal structure and various coupling constants in addition to the CF parameters. Values of some of the elastic constants are known for $TbVO_4$.[31] For $C_{33}$ and $C_{13}$ for which values are unavailable, the corresponding values for $ErVO_4$[39] were used in the present analysis.

TABLE II. The crystal-field parameters $B_n^m$ in units of $cm^{-1}$. The parameters for $TbPO_4$ defined in spherical tensor methods in Ref. 27 were converted to the representation in Steven's operator equivalents. The signs for $B_4^4$ and $B_6^4$ of $TbPO_4$ are opposite to those reported in Ref. 27 (see text).

| | $B_2^0$ | $B_4^0$ | $B_6^0$ | $B_4^4$ | $B_6^4$ | References |
|---|---|---|---|---|---|---|
| $TbVO_4$ | $-47.8$ | 33.3 | $-51.3$ | 757 | 54 | Present work |
| $TbPO_4$ | 178 | 14.9 | $-49.4$ | 835 | 83.6 | Ref. 27 |

The magnetoelastic coupling coefficients for the $\alpha 1$ and $\alpha 2$ strains can be obtained from a study of the thermal expansion above $T_D$. The magnetoelastic contribution to the thermal expansion has been estimated by comparing the temperature dependence of the lattice constants of $TbVO_4$[40,41] with that of $LuVO_4$. This method was applied successfully in the analysis of the thermal expansion of $HoVO_4$.[23] The contribution thus estimated was found to be proportional to the calculated value of $\langle O_2^0 \rangle$ in the entire temperature range above $T_D$. The proportionality coefficients can be expressed in terms of $B^{\alpha I}$ and $C_0^{\alpha i}$. The values of $B^{\alpha 1} = -2.9 \times 10^3$ cm$^{-1}$ and $B^{\alpha 2} = 4.2 \times 10^3$ cm$^{-1}$ were obtained. These values lead to the total coupling constant $G^{\alpha} = 20.3$ cm$^{-1}$. The calculated $T_D$ depends mainly on the coupling constant associated with $P_{xy}$ i.e., $G^{\delta}$. Its value was chosen to be 880 cm$^{-1}$ so that the calculation reproduces the experimental $T_D$. On the basis of the Hamiltonians in Eqs. (2) and (6), and using the coefficients stated above, we calculated the self-consistent value of $\langle P_{xy} \rangle$ and hence the order parameter $\varepsilon_{JT}^{\delta}$. The dashed line in Fig. 3 shows the temperature dependence of $\varepsilon_{JT}^{\delta}$ calculated for $TbVO_4$.

In order to describe the phase transition in the mixed crystals $TbV_{1-x}P_xO_4$, the change in the CF caused by phosphorous doping should be taken into account. The CF level structure for $TbPO_4$ was reported previously.[27] As was noted earlier, the most significant difference in the CF parameters for $TbVO_4$ and $TbPO_4$ is the opposite signs of the $B_2^0$ parameter. As far as the signs for $B_4^4$ and $B_6^4$ are concerned, a simultaneous change of their signs, which corresponds to a 45° rotation about the *c* axis, does not affect the CF level structure or transition strengths. Therefore, they were not determined unambiguously by the previous neutron-scattering experiment.[27] In the present treatment of magnetoelastic coupling, we chose the positive signs for $B_4^4$ and $B_6^4$ of $TbPO_4$, as listed in Table II. Similar analyses using the negative values for these parameters were found to give results inconsistent with observation. The choice of positive signs leads to values of the CF parameters for $TbPO_4$ that are not very different from those for $TbVO_4$ except for $B_2^0$. Since we are mainly concerned with crystals having a relatively small P doping, in the following analysis, the CF parameters, except for $B_2^0$, as well as all the coupling coefficients were assumed to have values equal to those of $TbVO_4$.

First, an oversimplified calculation was performed using the value of $B_2^0$ obtained by a linear interpolation between the corresponding values of the two pure compounds. For samples with smaller *x* value, the calculated $T_D$'s are higher by 3–8 K than those observed. As an example, the result of the calculation for $x = 0.18$ is shown by the dashed line against the experimental results in Fig. 6. Naturally, this approximation cannot be applied for P-rich crystals since only the variation in $B_2^0$ is considered in the calculations.

At the next level of sophistication, we have introduced a distribution of $B_2^0$ values as a truncated Gaussian function since the CF for Tb ions in the mixed crystals is expected to vary from site to site. The probability function is assumed to have a maximum at the linearly interpolated value of $B_2^0$.

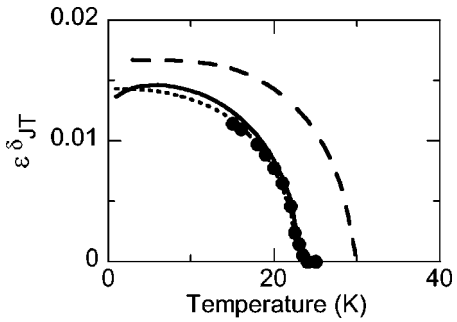


FIG. 6. The measured temperature dependence of $\varepsilon_{JT}^{\delta}$ for $x = 0.18$ (symbols) and results of the calculations based on several models. The dashed line represents the calculation using only the linearly interpolated value for $B_2^0$ ($-7.2$ cm$^{-1}$). The dotted line was obtained assuming a distribution in $B_2^0$. The solid line was calculated using the linearly interpolated value for $B_2^0$ (without distribution) and a distribution in $B_{xy}$ ($B_{xy-half} = 74$ cm$^{-1}$).

The truncation is based on the condition that $B_2^0$ cannot be smaller than that of $TbVO_4$ or greater than that of $TbPO_4$. The temperature dependence of $\varepsilon_{JT}^{\delta}$ was calculated based on these assumptions, and the result for $x = 0.18$ is shown by the dotted line in Fig. 6. However, in order to reproduce the experimental results, it was necessary to adjust the distribution function to favor excessively those $B_2^0$ values closer to that of $TbPO_4$.

Finally, we used an approach considering the *local* breaking of the tetragonal symmetry of the CF. Among the nontetragonal symmetry terms in the CF Hamiltonian, the one containing the operator $P_{xy}$ is expected to have a dominant influence on the Jahn-Teller effect. We write the corresponding CF parameter as $B_{xy}$, and add a term, $\alpha B_{xy} P_{xy}$ to the CF Hamiltonian of Eq. (2). The probability associated with the values of $B_{xy}$ is assumed to be a Gaussian function. The average value of $B_{xy}$ must be zero because the macroscopic tetragonal symmetry is retained. The half-width at half-maximum of the Gaussian function, denoted as $B_{xy-half}$, is chosen for each *x* so that the calculated and observed $T_D$ values agree. The calculation was performed using a single $B_2^0$ fixed by the linear interpolation according to the *x* value and the distribution in $B_{xy}$. The value of $B_{xy-half}$ assumed in the calculation varies from 56 cm$^{-1}$ for $x = 0.10$ to 87 cm$^{-1}$ for $x = 0.32$. The effect of this approach in calculating the temperature variation of the order parameter for the $x = 0.18$ sample is illustrated by the solid line in Fig. 6. The overall results for all the samples, as shown in Fig. 3, are in good agreement with the observed values of the order parameter. This result does not exclude the possibility that $B_2^0$ also has a distribution. As expected, by allowing a reasonable distribution in $B_2^0$ while reducing the distribution in $B_{xy}$, equally good agreement was obtained between the calculated and experimental results.

### C. Diffuse scattering

It is apparent that the diffuse scattering for $x = 0.32$ shown in Fig. 4(b) does not have the intensity distribution pattern of the TDS [Fig. 4(a)]. On the other hand, the intensity pattern

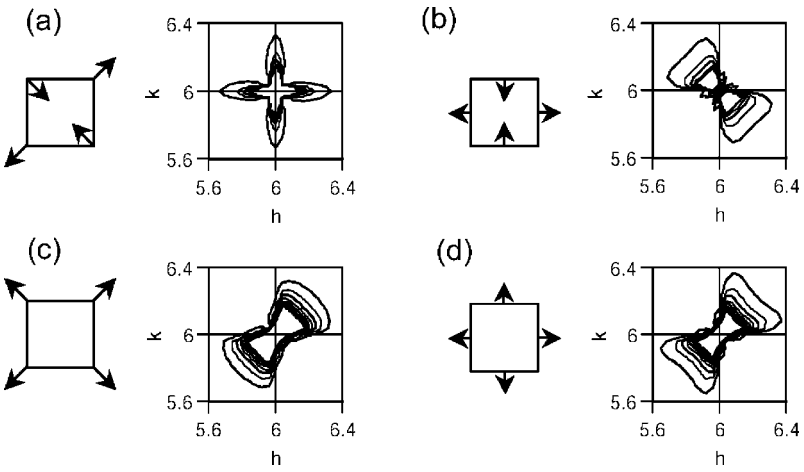


FIG. 7. Four examples of the calculated intensity distribution of the diffuse scattering due to different local strains.

obtained from a similar measurement for pure $TbVO_4$ at room temperature was found to be consistent with that of the TDS. As mentioned in Sec. III B, the presence of local strains in the mixed crystals modifies the CF on the Tb ions. In the case of $Tb(V,P)O_4$, the local strains such as $\varepsilon^{\alpha 1}$ and $\varepsilon^{\alpha 2}$ lead to varying values of $B_2^0$ whereas the local strain $\varepsilon^{\delta}$ contributes to the CF parameter $B_{xy}$ and its variation. We calculated the diffuse scattering patterns originating from these strains according to Ref. 42 around the (660) reciprocal point within the plane perpendicular to the $c^*$ axis. Figure 7 shows the symmetries of various types of strains and the corresponding intensity distribution patterns. The strain (a) has the same symmetry as the Jahn-Teller distortion $\varepsilon_{\mathrm{JT}}^{\delta}$, whereas the strains $\varepsilon^{\alpha 1}$ and $\varepsilon^{\alpha 2}$ correspond to a mixture of (c) and (d). Figures 7(a) and 7(b) show a very weak diffuse-scattering intensity along the (110) direction for the strains that do not introduce a volume change. The patterns of the scattering due to the strains with volume change, on the other hand, show substantial intensity extended along the (110) direction [Figs. 7(c) and 7(d)].

The observed diffuse scattering [Fig. 4(b)] clearly indicates the existence of strains with a volume change similar to those shown in Figs. 7(c) and 7(d). However, no conclusion can be reached regarding the existence of the strain $\varepsilon^{\delta}$ from the diffuse-scattering measurements since the intensity from this strain has essentially the same pattern as that of the TDS [Fig. 4(a)].

## V. CONCLUSIONS

We have studied the suppression of the cooperative Jahn-Teller effect in $TbV_{1-x}P_xO_4$ mixed crystals caused by the randomness introduced through a substitution of phosphorous atoms. The room-temperature lattice parameters of $TbV_{1-x}P_xO_4$ vary linearly with respect to $x$ over the full range of mixing concentrations. The transition temperature $T_{\mathrm{D}}$ in $TbV_{1-x}P_xO_4$ decreases with increasing P concentration. The reduction in $T_{\mathrm{D}}$ is more striking than that observed for $Tb(V,As)O_4$.[43] This appears to be due to the considerable difference in the CF of $TbVO_4$ and $TbPO_4$, and particularly to the opposite signs of the CF parameter $B_2^0$ and the large stains caused by the differing ionic radii of P and V. Calculations taking into account the distribution in $B_2^0$ revealed that the effects of such distribution alone do not explain the observed large reduction in $T_{\mathrm{D}}$. It is essential to include the effects of breaking the local symmetry due to the random distribution of the V and P atoms. We have introduced an additional operator $P_{xy}$ in the CF Hamiltonian with the corresponding CF parameter $B_{xy}$. The calculation that assumes a distribution of $B_{xy}$ values can explain the experimental order parameters satisfactorily for the $TbV_{1-x}P_xO_4$ system. Analyses on the basis of the pseudospin formalism were performed previously on the data for the Jahn-Teller transitions in (Tb, Tm) $VO_4$ and (Tb, Dy) $VO_4$.[11,12,17] In these analyses, the difference in the sizes of the rare-earth ions was assumed to give rise only to the local strain $\varepsilon^{\delta}$. The analysis performed in the present study is an extension through the use of an expanded Hamiltonian to calculate the changes in the wave functions due to the modified CF.

The observed pattern of the diffuse scattering intensity for $x=0.32$ suggests the existence of the strains $\varepsilon^{\alpha 1}$ and $\varepsilon^{\alpha 2}$. Such local strains should lead to the variation of the $B_2^0$ values. On the other hand, the existence of the strain $\varepsilon^{\delta}$ that contributes to the distribution in $B_{xy}$ values cannot be confirmed unambiguously. The magnitude of the magnetoelastic coupling constant $B^{\delta}$ is 3 to 4 times larger than those of $B^{\alpha 1}$ and $B^{\alpha 2}$. Therefore, even if the magnitude of the strain $\varepsilon^{\delta}$ is smaller than $\varepsilon^{\alpha 1}$ and $\varepsilon^{\alpha 2}$, it may result in a large variation in $B_{xy}$.

## ACKNOWLEDGMENTS

We thank K. Tajima for many helpful discussions and S. Skanthakumar for providing us the magnetic susceptibility data of $TbVO_4$. Work performed at Argonne National Laboratory and Oak Ridge National Laboratory was supported by the U.S. DOE, Basic Energy Sciences, under Contracts No. W-31-109-ENG-38 and No. DE-AC05-00OR22725, respectively. A part of this work was supported by Keio Kougakukai.

[1] B. C. Chakoumakos, M. M. Abraham, and L. A. Boatner, J. Solid State Chem. **109**, 197 (1994).
[2] W. G. Wyckoff, *Crystal Structure* (Wiley Interscience, New York, 1965), Vol. 3.
[3] G.A. Gehring and K.A. Gehring, Rep. Prog. Phys. **38**, 1 (1975).
[4] W. Nägele, D. Holhwein, and G. Domann, Z. Phys. B: Condens. Matter **39**, 305 (1980).
[5] R.T. Harley, W. Hayes, A.M. Perry, S.R.P. Smith, R.J. Elliott, and I.D. Saville, J. Phys. C **7**, 3145 (1974).
[6] G.A. Gehring, S.J. Swithenby, and M.R. Wells, Solid State Commun. **18**, 31 (1976).
[7] T.J. Glynn, R.T. Harley, and R.M. Macfarlane, J. Phys. C **10**, 2937 (1977).
[8] M. Schwab, Phys. Status Solidi B **86**, 195 (1978).
[9] D. Bingham, M.J. Morgan, and J.D. Cashion, Proc. Phys. Soc., London, Sect. A **391**, 85 (1984).
[10] A. Kasten, H.G. Kahle, and P. Klöfer, Solid State Commun. **52**, 725 (1984).
[11] A. Kasten, H.G. Kahle, P. Klöfer, and D. Schäfer-Siebert, Phys. Status Solidi B **144**, 423 (1987).
[12] G. Hess, M. Dammann, H.G. Kahle, A. Kasten, C. Seifert, and K. Vögtlin, J. Phys.: Condens. Matter **2**, 1073 (1990).
[13] A.V. Vasil'ev, A.E. Dvornikova, Z.A. Kazei, B.V. Mill, M.D. Kaplan, and V.I. Sokolov, Pis'ma Zh. Éksp. Teor. Fiz. **50**, 90 (1989) [JETP Lett. **50**, 103 (1989)].
[14] M.D. Kaplan and A.V. Vasilyev, Physica B **179**, 65 (1992).
[15] A.E. Dvornikova, M.D. Kaplan, Z.A. Kazei, B.V. Mill, V.I. Sokolov, and A.V. Vasilyev, Phys. Lett. A **147**, 139 (1990).
[16] V.I. Sokolov, M.D. Kaplan, Z.A. Kazei, A.V. Vasilyev, and A.E. Dvornikova, J. Phys. Chem. Solids **53**, 737 (1992).
[17] B. Pilawa, G. Hess, H.G. Kahle, and A. Kasten, Phys. Status Solidi B **145**, 729 (1988).
[18] J.T. Graham, J.H. Page, and D.R. Taylor, Phys. Rev. B **44**, 4127 (1991).
[19] K.A. Reza and D.R. Taylor, Phys. Rev. B **46**, 11 425 (1992).
[20] Z. Slanič, D.P. Belanger, J. Wang, and D.R. Taylor, Phys. Rev. B **53**, 97 (1996).
[21] C.-H. Choo, H.P. Schriemer, and D.R. Taylor, Phys. Rev. B **61**, 11 197 (2000).
[22] A.J. Dirkmaat, D. Huser, G.J. Nieuwenhuys, J.A. Mydosh, P. Kettler, and M. Steiner, Phys. Rev. B **36**, 352 (1987).
[23] S. Skanthakumar, C.-K. Loong, L. Soderholm, J.W. Richardson, Jr., M.M. Abraham, and L.A. Boatner, Phys. Rev. B **51**, 5644 (1995).
[24] K.A. Gehring, A.P. Malozemoff, W. Staude, and R.N. Tyte, Solid State Commun. **9**, 511 (1971).
[25] R.J. Elliott, R.T. Harley, W. Hayes, and S.R.P. Smith, Proc. Phys. Soc., London, Sect. A **328**, 217 (1972).
[26] K.W.H. Stevens, Proc. Phys. Soc., London, Sect. A **65**, 209 (1952).
[27] C.-K. Loong, L. Soderholm, G.L. Goodman, M.M. Abraham, and L.A. Boatner, Phys. Rev. B **48**, 6124 (1993).
[28] M. M. Abraham, L. A. Boatner, G. W. Beall, C. B. Finch, R. J. Floran, P. G. Huray, and M. Rappaz, *Alternate Nuclear Waste Forms and Interactions in Geologic Media* (U. S. Department of Energy, Gatlinburg, TN, 1980).
[29] K. Kirschbaum, A. Martin, D.A. Parrish, and A.A. Pinkerton, J. Phys.: Condens. Matter **11**, 4483 (1999).
[30] G. Venkataraman, L. A. Feldkamp, and V. C. Sahni, *Dynamics of Perfect Crystals* (The MIT Press, Cambridge, 1975).
[31] J.R. Sandercock, S.B. Palmer, R.J. Elliott, W. Hayes, S.R.P. Smith, and A.P. Young, J. Phys. C **5**, 3126 (1972).
[32] Z.A. Kazei, N.P. Kolmakova, A.A. Sidorenko, and L.A. Takunov, Fiz. Tverd. Tela (St. Petersburg) **40**, 1663 (1998) [Phys. Solid State **40**, 1513 (1998)].
[33] P. Morin, J. Rouchy, and D. Schmitt, Phys. Rev. B **37**, 5401 (1988).
[34] R.T. Harley, W. Hayes, and S.R.P. Smith, J. Phys. C **5**, 1501 (1972).
[35] M.-D. Guo, A.T. Aldred, and S.-K. Chan, J. Phys. Chem. Solids **48**, 229 (1987).
[36] G.A. Gehring, H.G. Kahle, W. Nägele, A. Simon, and W. Wüchner, Phys. Status Solidi B **74**, 297 (1976).
[37] S. Skanthakumar (unpublished).
[38] B.G. Vekhter, Z.A. Kazei, M.D. Kaplan, B.V. Mill', and V.I. Sokolov, Fiz. Tverd. Tela (Leningrad) **30**, 1021 (1988) [Sov. Phys. Solid State **30**, 592 (1998)].
[39] Y. Hirano, I. Guedes, M. Grimsditch, C.-K. Loong, N. Wakabayashi, and L.A. Boatner, J. Am. Ceram. Soc. **85**, 1001 (2002).
[40] Y. Hirano, N. Wakabayashi, C.-K. Loong, and L. A. Boatner (unpublished).
[41] Z.A. Kazei, N.P. Kolmakova, and O.A. Shishkina, Physica B **245**, 164 (1998).
[42] P.H. Dederichs, J. Phys. F: Met. Phys. **3**, 471 (1973).
[43] D.R. Taylor, D.J. Loken, and C.-H. Choo, J. Magn. Magn. Mater. **177-181**, 183 (1988).